A Class of Globally Stabilizing Feedback Controllers for the Orbital Rendezvous Problem

Mirko Leomanni*, Gianni Bianchini, Andrea Garulli, Antonio Giannitrapani

Dipartimento di Ingegneria dell'Informazione e Scienze Matematiche, Università di Siena, Siena, Italy

SUMMARY

The development of feedback control systems for autonomous orbital rendezvous is a key technological challenge for next generation space missions. This paper presents a new class of control laws for the orbital rendezvous problem. The controllers belonging to this class are guaranteed to globally asymptotically stabilize the relative dynamics of two satellites in circular or elliptic orbits. The proposed design procedure builds on control techniques for nonlinear systems in cascade form, by exploiting the geometric properties of the orbital element description of the satellite motion. A numerical simulation of a formation flying mission demonstrates the effectiveness of this approach for long-range and low-thrust rendezvous operations.

Received ...

KEY WORDS: Control applications; aerospace; orbital rendezvous; control design; Lyapunov methods

1. INTRODUCTION

Orbital rendezvous technologies play a fundamental role in interplanetary exploration, on-orbit servicing, and remote sensing space missions. They enable two spacecraft starting a long distance apart to get closer and perform activities such as inspection or docking. Historically, rendezvous maneuvers have been performed through manual or semi-automated procedures [1]. Despite the success of these methods, they are not suited to applications in which ground communication is limited or delayed, and often very expensive to implement [2]. For these reasons, the development of fully autonomous rendezvous techniques has been identified as a key challenge for current and future formation flying missions, see, e.g., [3, 4, 5].

The rendezvous control problem can be tackled by using open-loop optimization techniques or feedback stabilization methods. In the former approach, no closed-form solution is available in general and a two-point boundary value problem is solved numerically to obtain the optimal thrusting profile (see, e.g., [6, 7, 8]). The related computations are lengthy, thus making this approach not suitable for applications in which the control signal must be computed online. On the contrary, feedback stabilization methods typically provide closed-form control laws, that can be employed within an autonomous guidance, navigation and control system.

Many of the rendezvous control schemes discussed in the formation flying literature rely on results from linear control theory. Linear quadratic regulator design techniques are adopted in [9, 10, 11]. A robust control problem is addressed in [12, 13], by using H_∞ synthesis methods. Model predictive control strategies, able to cope with both input and state constraints, are presented in [14, 15, 16, 17]. Unfortunately, most of these approaches are based on linearized, time-invariant dynamic models, which limits the domain of attraction of the control system to a local neighborhood

*Correspondence to: leomanni@diism.unisi.it

of the rendezvous location. In order to mitigate this issue, linear time-varying controllers have been presented in [18, 19]. These approaches require to solve numerically a periodic Riccati equation or a parametric Lyapunov equation.

Several nonlinear control techniques have also been considered in the literature. Feedback linearization is proposed in early works such as [20, 21]. Adaptive control schemes, accounting for both parametric uncertainties and unknown disturbances, are presented in [22, 23, 24, 25]. In these approaches, the control input is chosen so as to exactly cancel or to dominate the effect of differential gravity (i.e., the difference between the gravitational accelerations acting on the two spacecraft). This can lead to a large control effort and consequently to poor fuel efficiency, especially when the relative position error is large. Hence, constraints on the maximum thrust that can be delivered by the actuators and on the amount of available propellant may restrict the applicability of these controllers to short-range maneuvers. In order to deal with input and state constraints, approaches based on nonlinear model predictive control and receding-horizon strategies have been proposed (see, e.g., [26, 27, 28]). These techniques are usually computationally intensive, as they require to solve a nonlinear optimal control problem at each time step. Moreover, it is often difficult to prove the stability of these methods.

In [29], a nonlinear Lyapunov-based control law is obtained by parameterizing the satellite relative motion in terms of orbital element differences. It is found that, in this way, the control energy can be made significantly smaller than the one resulting from the application of cartesian feedback control laws, such as those cited above. The authors, however, recognize that their design is not supported by a rigorous stability proof. A similar approach is taken in [30], where backstepping and forwarding techniques are adopted to derive a passivity-based controller. This control strategy applies only to perfectly circular reference orbits, which leaves out many scenarios of theoretical and practical interest. It is known, for instance, that low Earth orbits cannot have zero eccentricity, due to the asymmetry of the Earth's gravity field. Other control schemes based on orbital elements can be found in the literature [31, 32, 33]. However, they do not address the tracking of the satellite phase angle along the orbit, and hence cannot be employed for rendezvous.

In this paper, a new class of orbital element feedback control laws is presented for the rendezvous problem. The controllers belonging to this class are guaranteed to globally asymptotically stabilize the relative dynamics of a satellite pair, for both circular and elliptic reference orbits. Our design procedure is in the spirit of previous studies dealing with the global stabilization of nonlinear time-varying systems in cascade form, see, e.g., [34, 35, 36]. A set of tunable design functions is introduced to parameterize the stabilizing controller family. Such parametrization may be exploited to enforce further control specifications, or to optimize suitable performance indices. A simulation case study is presented in order to demonstrate the applicability of the proposed method. It is observed that, by applying the proposed design, the thrust command can be scaled down to meet the constraints dictated by modern low-thrust actuator technologies, such as electric propulsion. A qualitative robustness analysis with respect to environmental disturbances and parametric uncertainties is also carried out. A preliminary version of this work has been presented in [37].

The paper is organized as follows. In Section 2, a brief introduction to the orbital element parametrization is given and the considered rendezvous control problem is formulated. Section 3 is devoted to the controller design, which is demonstrated by the numerical case study in Section 4. Some concluding remarks are outlined in Section 5.

Notation

The notation is fairly standard. $\mathbb{R}^n$ is the real $n-$space, and $\mathbb{Z}$ denotes the set of integer numbers; for a real vector or matrix x, x^T denotes its transpose. The symbol $0_{n\times m}$ denotes a null matrix or vector with n rows and m columns, while the identity matrix of order n is denoted by I_n. The partial derivative $\partial f/\partial x$ is expressed as a row vector. To save space, $\cos(\cdot)$, $\sin(\cdot)$ are abbreviated with $\mathrm{c}(\cdot)$ and $\mathrm{s}(\cdot)$, respectively. Moreover,

$$R(\phi) = \begin{bmatrix} \mathrm{c}(\phi) & -\mathrm{s}(\phi) \\ \mathrm{s}(\phi) & \mathrm{c}(\phi) \end{bmatrix}$$

is the counter-clockwise rotation operator, by an angle ϕ, in $\mathbb{R}^2$. The definition of the signum function follows the convention

$$\text{sgn}(x) = \begin{cases} 1 & x > 0 \\ 0 & x = 0 \\ -1 & x < 0\,, \end{cases}$$

where $x \in \mathbb{R}$. The continuous time index is denoted by $t \in \mathbb{R}^+$.

2. PROBLEM FORMULATION

Classical orbital elements are commonly used as a parametrization of the position $r \in \mathbb{R}^3$ and velocity $\dot{r} \in \mathbb{R}^3$ of an orbiting body, since they provide a clear physical insight of the body motion. The semi-major axis $a > 0$ and eccentricity $e \in [0, 1]$ define the shape of the orbit. The inclination $i \in [0, \pi]$ and longitude of the ascending node $\Omega \in [0, 2\pi]$ define the orientation of the orbital plane with respect to a given inertial, right-handed reference frame centered at the central body (e.g., the Earth). The argument of perigee $\omega \in [0, 2\pi]$ describes the position of the perigee in the orbital plane, and the true anomaly $\nu(t) \in [0, 2\pi]$ defines the instantaneous angle at which the orbiting body is located relative to the perigee position, as illustrated in Fig. 1.

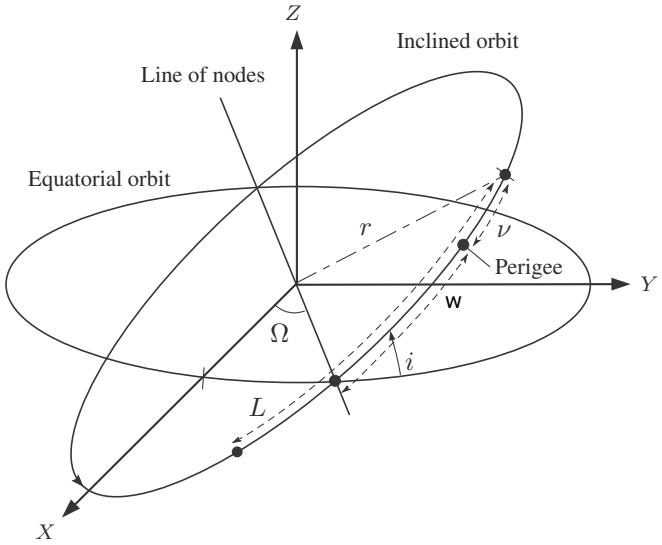

Figure 1. Classical orbital elements.

It is well known that ω is indeterminate for circular orbits (i.e., when $e = 0$) and Ω is indeterminate for equatorial orbits (i.e., when $i = 0$). These singularities can be avoided by adopting a different parameterization of the orbit using the modified equinoctial elements $\psi = [\psi_1 \ \ldots \ \psi_6]^T$, defined as [38]

$$\begin{array}{rcll} \psi_1 & = & L & = \ \Omega + \omega + \nu \\ \psi_2 & = & p & = \ a(1 - e^2) \\ \psi_3 & = & e_X & = \ e\ \text{c}(\Omega + \omega) \\ \psi_4 & = & e_Y & = \ e\ \text{s}(\Omega + \omega) \\ \psi_5 & = & h_X & = \ \tan(i/2)\,\text{c}(\Omega) \\ \psi_6 & = & h_Y & = \ \tan(i/2)\,\text{s}(\Omega). \end{array} \tag{1}$$

In this parameterization, L is the true longitude shown in Fig. 1, p is the orbit semi-parameter, e_X, e_Y are the components of the eccentricity vector, and h_X, h_Y are the components of the inclination vector. Notice that any closed Keplerian orbit is such that $\psi_2 = p > 0$. Moreover, the escape to parabolic orbits (i.e., $e = 1$) is not possible with continuous feedback [33], which is the

case considered in this paper. Therefore, in the following we restrict our attention to the case $e < 1$. Hence, the orbital element vector ψ must belong to the set

$$\Psi = \{\psi \in \mathbb{R}^6 : \ \psi_2 > 0, \ \ \psi_3^2 + \psi_4^2 < 1\}. \tag{2}$$

The transformation that relates the equinoctial elements to the cartesian position r and velocity $\dot{r}$, expressed in the inertial frame XYZ, can be found in astrodynamics textbooks (e.g., [39]), and is not reported here for brevity.

The dynamics of the orbital elements ψ in (1), in the presence of perturbing accelerations, are described by the Gauss' variational equations. Let us introduce the input vector $u = [u_r \ u_\theta \ u_h]^T$, where u_r, u_θ and u_h denote the radial, tangential and normal components of the acceleration, respectively, in a local-vertical-local-horizontal (LVLH) frame centered at the orbiting body. The resulting dynamics are given by ([39], Chapter 10)

$$\dot{\psi} = f(\psi) + g(\psi)u, \tag{3}$$

where the vector fields $f(\psi)$ and $g(\psi)$ are defined as

$$f(\psi) = \sqrt{\frac{\mu}{\psi_2^3}} \ \begin{bmatrix} (1+\zeta_X)^2 & 0 & 0 & 0 & 0 & 0 \end{bmatrix}^T \tag{4}$$

$$g(\psi) = \frac{\sqrt{\psi_2}}{\sqrt{\mu}(1+\zeta_X)} \begin{bmatrix} 0 & 0 & \eta \\ 0 & 2\,\psi_2 & 0 \\ (1+\zeta_X)\,\mathrm{s}(\psi_1) & q_X & -\eta\,\psi_4 \\ -(1+\zeta_X)\,\mathrm{c}(\psi_1) & q_Y & \eta\,\psi_3 \\ 0 & 0 & \dfrac{(1+h^2)}{2}\,\mathrm{c}(\psi_1) \\ 0 & 0 & \dfrac{(1+h^2)}{2}\,\mathrm{s}(\psi_1) \end{bmatrix}, \tag{5}$$

μ is the gravitational parameter of the central body, and

$$\begin{aligned} \zeta_X &= e\ \mathrm{c}(\nu) = \psi_3\,\mathrm{c}(\psi_1) + \psi_4\,\mathrm{s}(\psi_1) \\ q_X &= \psi_3 + (2+\zeta_X)\,\mathrm{c}(\psi_1) \\ q_Y &= \psi_4 + (2+\zeta_X)\,\mathrm{s}(\psi_1) \\ \eta &= \psi_5\,\mathrm{s}(\psi_1) - \psi_6\,\mathrm{c}(\psi_1) \\ h^2 &= \psi_5^2 + \psi_6^2. \end{aligned}$$

Most rendezvous applications involve a maneuvering spacecraft, called the *chaser*, and a passive one, which is referred to as the *target* [40]. Let $\psi(t)$ be the state of the chaser spacecraft. The control objective of the chaser is to track the known trajectory of the target, specified by the orbital elements $\psi^r(t) = [\psi_1^r, \ldots, \psi_6^r]^T$. It is assumed that the target spacecraft moves along an unperturbed orbit. Consequently, the target dynamics are represented by equation (3) with $u = 0$, i.e.,

$$\dot{\psi^r} = f(\psi^r). \tag{6}$$

It can be seen from (4) and (6) that the target phase angle $\psi_1^r(t)$ is time-varying, while $\psi_2^r, \ldots, \psi_6^r$ are constants that define the shape and orientation of the reference orbit.

The tracking error is defined as $\tilde{\psi} = \psi - \psi^r$. Hence, the error dynamics evolve according to the nonlinear time-varying system

$$\dot{\tilde{\psi}} = \tilde{f}(\tilde{\psi}, \psi^r) + g(\tilde{\psi} + \psi^r)u, \tag{7}$$

where $\tilde{f}(\tilde{\psi}, \psi^r) = f(\tilde{\psi} + \psi^r) - f(\psi^r)$.

The orbital rendezvous problem considered in this paper can be formulated as follows.

Problem 1
Find a class $\mathcal{U}$ of continuous state feedback control laws $u = u(\tilde{\psi}, \psi^r)$ such that the origin of the error system (7) is globally asymptotically stable, which guarantees that

$$\lim_{t\to\infty} \tilde{\psi}(t) = 0$$

for any initial condition $\tilde{\psi}(0) = \psi(0) - \psi^r(0)$, with $\psi(0) \in \Psi$ and $\psi^r(0) \in \Psi$.

3. MAIN RESULTS

In order to derive a solution to Problem 1, we first introduce a coordinate transformation $x = x(\tilde{\psi}, \psi^r)$ in system (7), defined as follows

$$\begin{aligned}
x_1 &= \tilde{\psi}_1 \\
x_2 &= \sqrt{1 + \frac{\tilde{\psi}_2}{\psi_2^r}} - 1 \\
\begin{bmatrix} x_3 \\ x_4 \end{bmatrix} &= \begin{bmatrix} \frac{\psi_2^r}{\tilde{\psi}_2 + \psi_2^r} & 0 \\ 0 & \sqrt{\frac{\psi_2^r}{\tilde{\psi}_2 + \psi_2^r}} \end{bmatrix} R(\tilde{\psi}_1 + \psi_1^r) \begin{bmatrix} \tilde{\psi}_3 + \psi_3^r \\ -\tilde{\psi}_4 - \psi_4^r \end{bmatrix} + \begin{bmatrix} -\frac{\tilde{\psi}_2}{\tilde{\psi}_2 + \psi_2^r} \\ 0 \end{bmatrix} - \begin{bmatrix} \zeta_X^r \\ \zeta_Y^r \end{bmatrix} \\
x_5 &= \tilde{\psi}_5 \\
x_6 &= \tilde{\psi}_6,
\end{aligned} \tag{8}$$

where

$$\begin{bmatrix} \zeta_X^r \\ \zeta_Y^r \end{bmatrix} = R(\psi_1^r) \begin{bmatrix} \psi_3^r \\ -\psi_4^r \end{bmatrix}.$$

A similar transformation is used in [30] for the case of circular reference orbits (i.e., $\zeta_X^r = \zeta_Y^r = 0$). System (7) in the new coordinate set takes on the form

$$\dot{x} = \begin{bmatrix} F(\chi, \psi^r) \\ 0_{2\times 1} \end{bmatrix} + \begin{bmatrix} G(\chi, \psi^r) \\ 0_{2\times 2} \end{bmatrix} \begin{bmatrix} u_r \\ u_\theta \end{bmatrix} + H(x, \psi^r)\, u_h\,, \tag{9}$$

where $\chi = [x_1 \dots x_4]^T$ and

$$F(\chi, \psi^r) = \begin{bmatrix} 0 & F_{12} & F_{13} & 0 \\ 0 & 0 & 0 & 0 \\ 0 & 0 & -F_{33} & -F_{12} \\ 0 & F_{42} & F_{12}+F_{43} & 0 \end{bmatrix} \chi$$

$$G(\chi, \psi^r) = \begin{bmatrix} 0 & 0 \\ 0 & G_{22} \\ 0 & 0 \\ G_{41} & 0 \end{bmatrix},$$

being

$$
\begin{aligned}
F_{12} &= \sqrt{\frac{\mu}{(\psi_2^r)^3}}\,(x_3+1+\zeta_X^r)^2\\
F_{13} &= \sqrt{\frac{\mu}{(\psi_2^r)^3}}\,(x_3+2+2\zeta_X^r)\\
F_{42} &= \sqrt{\frac{\mu}{(\psi_2^r)^3}}\,(x_2+2)\,(x_3+1+\zeta_X^r)^3\\
F_{33} &= F_{13}\,\zeta_Y^r\\
F_{43} &= F_{13}\,\zeta_X^r\\
G_{22} &= \sqrt{\frac{\psi_2^r}{\mu}}\,\frac{1}{(x_3+1+\zeta_X^r)}\\
G_{41} &= \sqrt{\frac{\psi_2^r}{\mu}}.
\end{aligned}
$$

By virtue of the properties of the considered problem (see (2)), all F_{ij} and G_{ij} are strictly positive functions of χ and ψ^r, except for F_{33} and F_{43}. The vector $H(x,\psi^r)$ in (9) is given by

$$
H(x,\psi^r)=\frac{\partial x}{\partial \tilde{\psi}}\,g_h(\psi)=\frac{G_{22}}{(x_2+1)}\begin{bmatrix}(x_5+\psi_5^r)\,\mathrm{s}(x_1+\psi_1^r)-(x_6+\psi_6^r)\,\mathrm{c}(x_1+\psi_1^r)\\ 0_{3\times 1}\\ \dfrac{1+(x_5+\psi_5^r)^2+(x_6+\psi_6^r)^2}{2}\,\mathrm{c}(x_1+\psi_1^r)\\ \dfrac{1+(x_5+\psi_5^r)^2+(x_6+\psi_6^r)^2}{2}\,\mathrm{s}(x_1+\psi_1^r)\end{bmatrix} \tag{10}
$$

where $g_h(\cdot)$ denotes the third column of $g(\cdot)$ in (5). It can be verified that the vector fields $F(\chi,\psi^r)$, $G(\chi,\psi^r)$ and $H(x,\psi^r)$ in (9) are periodic in $\psi^r(t)$, and turn out to be periodic also in t, with period equal to the reference orbital period

$$
T=2\,\pi\sqrt{\frac{(\psi_2^r)^3}{\mu\,[1-(\psi_3^r)^2-(\psi_4^r)^2]^3}}. \tag{11}
$$

The structure of system (9) allows us to tackle the control design problem in a two-step procedure. The first step is equivalent to solving a co-planar rendezvous problem, by controlling the χ components of system (9) with the inputs u_r and u_θ. This is accomplished by applying a backstepping-inspired technique. The second step amounts to asymptotically stabilizing the x_5, x_6 components of system (9) with the input u_h, while retaining the asymptotic stability of the χ components. The proposed approach is described in detail in the following.

3.1. Step 1

In this step, we assume $u_h = 0$ in (9) and derive a feedback stabilizer for the fourth order subsystem

$$
\dot{\chi}=F(\chi,\psi^r)+G(\chi,\psi^r)\begin{bmatrix}u_r\\ u_\theta\end{bmatrix} \tag{12}
$$

using the inputs u_r and u_θ.

For system (12), let us first introduce the following nonsingular transformation in the input variables

$$u_r = \frac{1}{G_{41}}\left(v_r - F_{43}x_3\right) \tag{13}$$

$$u_\theta = \frac{1}{G_{22}}\left(v_\theta - F_{12}\frac{\partial \lambda_1}{\partial x_1}\right), \tag{14}$$

where v_r and v_θ are the new input variables, and $\lambda_1 = \lambda_1(x_1)$ is a given positive-definite and pseudoconvex function of class C^2, to be treated as a design parameter. Then, system (12) becomes

$$\dot{x}_1 = F_{12}x_2 + F_{13}x_3 \tag{15}$$

$$\dot{x}_2 = -F_{12}\frac{\partial \lambda_1}{\partial x_1} + v_\theta \tag{16}$$

$$\dot{x}_3 = -F_{33}x_3 - F_{12}x_4 \tag{17}$$

$$\dot{x}_4 = F_{42}x_2 + F_{12}x_3 + v_r. \tag{18}$$

Let

$$x_4^* = \frac{1}{F_{12}}\left(\frac{F_{13}}{\lambda_5}\frac{\partial \lambda_1}{\partial x_1} - F_{33}x_3 + \lambda_3\right), \tag{19}$$

where λ_5 is a positive constant, and $\lambda_3 = \lambda_3(x)$ is a given function of class C^1 satisfying $\mathrm{sgn}(\lambda_3) = \mathrm{sgn}(x_3)$. Similarly to backstepping control design (see, e.g., [41]), we use x_4^* as a virtual input for system (15)-(17), and consider the transformed state vector

$$z = [z_1 \;\; z_2 \;\; z_3 \;\; z_4]^T = [x_1 \;\; x_2 \;\; x_3 \;\; (x_4 - x_4^*)]^T. \tag{20}$$

In the new coordinates, equations (15)-(18) read

$$\dot{z}_1 = F_{12}z_2 + F_{13}z_3 \tag{21}$$

$$\dot{z}_2 = -F_{12}\frac{\partial \lambda_1}{\partial z_1} + v_\theta \tag{22}$$

$$\dot{z}_3 = -\frac{F_{13}}{\lambda_5}\frac{\partial \lambda_1}{\partial z_1} - F_{12}z_4 - \lambda_3 \tag{23}$$

$$\dot{z}_4 = F_{42}z_2 + F_{12}z_3 + v_r - \dot{x}_4^*, \tag{24}$$

where clearly $\lambda_1(z_1) = \lambda_1(x_1)$. The following theorem addresses the global stabilization of system (21)-(24), and, equivalently, of (12).

Theorem 1
Let the control inputs of system (12)-(14) be given as

$$v_r = \dot{x}_4^* - \lambda_4 \tag{25}$$

$$v_\theta = -F_{42}\,\lambda_5\,z_4 - \lambda_2, \tag{26}$$

where $\lambda_2 = \lambda_2(z)$ and $\lambda_4 = \lambda_4(z)$ are given functions of class C^0 satisfying $\mathrm{sgn}(\lambda_2) = \mathrm{sgn}(z_2)$ and $\mathrm{sgn}(\lambda_4) = \mathrm{sgn}(z_4)$, respectively. Then, the equilibrium point $\chi = 0$ of the closed-loop system (12)-(14) with the control inputs (25)-(26) is uniformly globally asymptotically stable.

Proof
Consider the Lyapunov function candidate

$$V_1(z) = \lambda_1(z_1) + \frac{1}{2}z_2^2 + \frac{\lambda_5}{2}\left(z_3^2 + z_4^2\right). \tag{27}$$

The time derivative of (27), along the trajectories of (21)-(24), reads

$$\dot{V}_1(z) = (v_\theta + F_{42}\lambda_5 z_4)z_2 - \lambda_5\lambda_3 z_3 + \lambda_5(v_r - \dot{x}_4^*)z_4. \tag{28}$$

By substituting (25)-(26) in (28), one gets

$$\dot{V}_1(z) = -\lambda_2 z_2 - \lambda_5\lambda_3 z_3 - \lambda_5\lambda_4 z_4. \tag{29}$$

Clearly, (29) is negative semidefinite and vanishes for $z_2 = z_3 = z_4 = 0$. From (21), the latter condition implies that z_1 is constant. Moreover, since $\lambda_1(z_1)$ is pseudoconvex, $\partial\lambda_1/\partial z_1$ in (22)-(23) vanishes if and only if $z_1 = 0$. Combining these observations, it follows that the largest invariant set in which $\dot{V}_1 = 0$ is $z = 0$. Being system (21)-(26) periodic, by invoking LaSalle's principle for periodic systems ([42], Theorem 5.26), one has that $z = 0$ is globally uniformly asymptotically stable. Then, since the coordinate transformation (20) is diffeomorphic and $\chi = 0$ if and only if $z = 0$, it can be concluded that the equilibrium point $\chi = 0$ is globally asymptotically stabilized by the proposed control scheme. □

3.2. Step 2

The stabilization of the full system can be tackled by substituting into (9) the control inputs u_r, u_θ defined by (13)-(14) and (25)-(26), and rewriting the resulting dynamics as

$$\dot{x} = \begin{bmatrix} F_{cl}(\chi, \psi^r) \\ 0_{2\times 1} \end{bmatrix} + H(x, \psi^r)\, u_h, \tag{30}$$

where

$$F_{cl}(\chi, \psi^r) = \begin{bmatrix} F_{12}x_2 + F_{13}x_3 \\ -F_{12}\frac{\partial\lambda_1}{\partial x_1} - F_{42}\,(x_4 - x_4^*)\lambda_5 - \lambda_2 \\ -F_{13}\frac{1}{\lambda_5}\frac{\partial\lambda_1}{\partial x_1} - F_{12}(x_4 - x_4^*) - \lambda_3 \\ F_{42}x_2 + F_{12}x_3 + \dot{x}_4^* - \lambda_4 \end{bmatrix}.$$

Given the structure of (30), it turns out that the origin of the system can be globally stabilized using u_h via a damping-like controller, as stated by the next result.

Theorem 2
Consider the Lyapunov function candidate

$$V(x, \psi^r) = V_1(z) + \frac{1}{2}x_5^2 + \frac{1}{2}x_6^2, \tag{31}$$

with V_1 defined by (27) and z as in (20). Let

$$u_h = -\lambda_6, \tag{32}$$

where $\lambda_6 = \lambda_6(x, \psi^r)$ is a given function of class C^0 satisfying

$$\text{sgn}(\lambda_6) = \text{sgn}\left(\frac{\partial V(x, \psi^r)}{\partial x}\, H(x, \psi^r)\right). \tag{33}$$

Then, the equilibrium point $x = 0$ of the closed-loop system (30) with the control input (32) is uniformly globally asymptotically stable.

Proof
The time derivative of (31), along the trajectories of (30),(32), can be written as

$$\begin{aligned}\dot{V}(x, \psi^r) &= \frac{\partial V(x, \psi^r)}{\partial x}\begin{bmatrix} F_{cl}(\chi, \psi^r) \\ 0_{2\times 1} \end{bmatrix} + \frac{\partial V(x, \psi^r)}{\partial \psi^r} f(\psi^r) - \frac{\partial V(x, \psi^r)}{\partial x} H(x, \psi^r)\lambda_6 \\ &= \dot{V}_1(z) - \frac{\partial V(x, \psi^r)}{\partial x} H(x, \psi^r)\lambda_6,\end{aligned}$$

where $\dot{V}_1(z)$ is given by (29). Notice that $\dot{V}$ is negative semidefinite and vanishes if and only if

$$\begin{cases} x_2 = x_3 = 0 \\ x_4 = x_4^* \\ \dfrac{\partial V(x,\psi^r)}{\partial x} H(x,\psi^r) = 0. \end{cases} \tag{34}$$

The above conditions imply $u_h = 0$. By substituting (32) in (30) and enforcing (34), the closed-loop system becomes,

$$\dot{x} = \begin{bmatrix} 0 \\ -F_{12}\,\partial\lambda_1/\partial x_1 \\ -F_{13}\,\lambda_5^{-1}\,\partial\lambda_1/\partial x_1 \\ \dot{\gamma} \\ 0_{2\times 1} \end{bmatrix}, \tag{35}$$

where $\gamma = \gamma(x_1, \psi^r)$ is obtained from (19) as

$$\gamma = \lambda_5^{-1} \frac{F_{13}}{F_{12}} \frac{\partial \lambda_1}{\partial x_1}.$$

Clearly, the only solution of system (35) satisfying the first two conditions in (34) is such that $\chi = 0$. Hence, according to Theorem 1, the set $\chi = 0$ is invariant. Moreover, x_5 and x_6 are constant along the solutions of (35). By using (10), for $\chi = 0$ one gets

$$\frac{\partial V(x,\psi^r)}{\partial x} H(x,\psi^r) = \sqrt{\frac{\psi_2^r}{\mu}} \frac{[1 + (x_5 + \psi_5^r)^2 + (x_6 + \psi_6^r)^2]}{2(1+\zeta_X^r)} \left[x_5\, \mathrm{c}(\psi_1^r) + x_6\, \mathrm{s}(\psi_1^r)\right].$$

Being $\psi_2^r > 0$, $1 + \zeta_X^r > 0$ and $\dot{\psi}_1^r \neq 0$, one must have $x_5 = x_6 = 0$ in order for the third condition in (34) to hold. Summarizing, the largest invariant set in which $\dot{V} = 0$ is $x = 0$. Then, by invoking LaSalle's principle for periodic systems, one has that that the proposed control strategy renders the equilibrium point $x = 0$ of system (30) globally uniformly asymptotically stable. □

The final expression of the control $u = [u_r, u_\theta, u_h]^T$ is obtained from (13)-(14), (20), (25)-(26) and (32) as

$$u_r = u_r(x, \psi^r; \lambda) = -\frac{1}{G_{41}} \left(F_{43}\, x_3 - \dot{x}_4^*\right) - \frac{\lambda_4}{G_{41}} \tag{36}$$

$$u_\theta = u_\theta(x, \psi^r; \lambda) = -\frac{F_{12}}{G_{22}} \frac{\partial \lambda_1}{\partial x_1} - \frac{F_{42}}{G_{22}} (x_4 - x_4^*)\lambda_5 - \frac{\lambda_2}{G_{22}} \tag{37}$$

$$u_h = u_h(x, \psi^r; \lambda) = -\lambda_6, \tag{38}$$

with x_4^* given by (19) and $V(x, \psi^r)$ defined by (31).

Expressions (36)-(38) define a class of globally stabilizing feedback controllers parameterized by the tunable vector-valued function $\lambda : \mathbb{R}^6 \times \mathbb{R}^6 \to \mathbb{R}^6$. Indeed, let

$$\Lambda = \left\{ \begin{bmatrix} \lambda_1 \\ \vdots \\ \lambda_6 \end{bmatrix} : \begin{array}{ll} \lambda_1 \in C^2 & \text{positive definite,} \\ & \frac{\partial \lambda_1}{\partial x_1} = 0 \Leftrightarrow x_1 = 0 \\ \lambda_2 \in C^0 & : \mathrm{sgn}(\lambda_2) = \mathrm{sgn}(x_2) \\ \lambda_3 \in C^1 & : \mathrm{sgn}(\lambda_3) = \mathrm{sgn}(x_3) \\ \lambda_4 \in C^0 & : \mathrm{sgn}(\lambda_4) = \mathrm{sgn}(x_4 - x_4^*) \\ \lambda_5 > 0 & \text{constant} \\ \lambda_6 \in C^0 & : \mathrm{sgn}(\lambda_6) = \mathrm{sgn}(\frac{\partial V}{\partial x} H) \end{array} \right\}.$$

Then, the controller class

$$\mathcal{U} = \left\{\, u(x, \psi^r; \lambda) \;:\; \lambda \in \Lambda \,\right\} \tag{39}$$

is a solution to Problem 1.

Finally, note that $\mathcal{U}$ can be further generalized by taking λ_5 as a strictly positive function, with minor amendments of the control law (36)-(38).

Remark 1
The degrees of freedom provided by the proposed controller class, i.e., by the tunable parameters $\lambda \in \Lambda$, can be used to enforce further control specifications or to meet given performance requirements. A typical specification in aerospace applications is to keep the magnitude of the thrust command within the safe operating range of the satellite engines. Notice that this is a very simple task for circular reference orbits ($F_{33} = F_{43} = 0$), as it amounts to properly scale the tuning functions λ. The problem is more challenging for elliptical reference orbits, due to the presence of the term $(F_{43}x_3 - \dot{x}_4^*)$ in (36). An example that demonstrates the tuning of λ for a specific case study is presented in the next section. A systematic method for exploiting the proposed parameterization in order to optimize relevant performance indices is the subject of current investigation.

Remark 2
Although $\mathcal{U}$ is a global stabilizer for Problem 1, it can lead to unwinding when applied to the physical system (7), in which the configuration space of the rotational degree of freedom $\tilde{\psi}_1$ is the unit circle [43]. A possible way to overcome this issue is suitably amend the definition of λ_1, by choosing e.g. $\lambda_1(x_1) = \kappa(1 - \mathrm{c}(x_1))$, where $\kappa > 0$. Notice that this introduces a set of unstable equilibrium points in the closed-loop system dynamics, corresponding to $x_1 = \pi + 2m\pi$, with $m \in \mathbb{Z}$. In this setting, only almost global stability can be guaranteed by adopting a reasoning similar to Theorems 1 and 2.

4. RENDEZVOUS CASE STUDY

In order to validate the proposed approach, a simulation model based on Cowell's formulation [39] has been implemented. In this model, the plant dynamics are given by

$$\begin{cases} \ddot{r} &= -\dfrac{\mu}{\|r\|^3} r + u_I + d \\ \ddot{r}^r &= -\dfrac{\mu}{\|r^r\|^3} r^r + d^r \end{cases} \tag{40}$$

where r and r^r denote the inertial position of the chaser and the target, respectively, and u_I is the control input of the chaser, expressed in the inertial frame. Moreover, the two vectors d and d^r in (40) represent environmental perturbations (e.g., aspherical gravity). These are treated as exogenous disturbances to be rejected by the control system. The proposed control law is applied to system (40) by first converting $r, \dot{r}$ and $r^r, \dot{r}^r$ into orbital elements and then rotating the input vector u given by (36)-(38) from the LVLH frame to the inertial frame. The resulting closed-loop system is shown in Fig. 2.

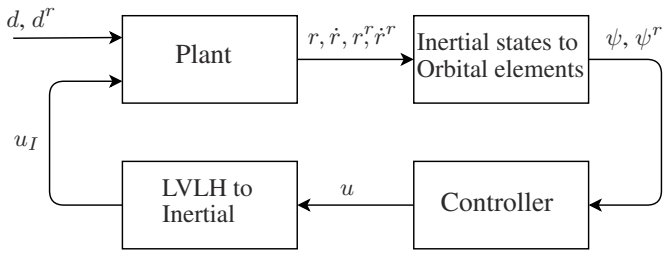

Figure 2. Block diagram of the closed-loop system (36)-(38), (40).

The considered rendezvous case study involves an actively controlled chaser spacecraft that must intercept a non-maneuvering target spacecraft, by using continuous, low-thrust propulsion. Both

spacecraft are released in a near-circular orbit with an altitude of about 800 km above the Earth, which is a typical setting for remote sensing missions. Their initial orbital elements are reported in Table I, and correspond to the relative position error

$$y(0) = [-21, 102, 71]^T \text{ km},$$

where $y(t) = r(t) - r^r(t)$. The settling time for the rendezvous maneuver is defined as

$$\bar{t} : \forall t > \bar{t} \ \ \|y(t)\| \leq 1\,\text{km},$$

where the relative distance of 1 km typically marks the transition from the rendezvous phase to the close proximity phase [40]. It is required to keep the maximum input magnitude in the order of 1 mm/s^2, for the given initial condition. This value is compatible with the characteristics of missions equipped with low-thrust propulsion technologies [44, 45].

In order to meet the control specifications, the following choices have been made for the tuning functions λ, by adopting a trial-and-error procedure:

$$\begin{aligned}
\lambda_1 &= 10^{-4} \cdot x_1^2 \\
\lambda_2 &= 10^{-8} \cdot \text{atan}(10^4 \cdot x_2) \\
\lambda_3 &= 10^{-3} \cdot x_3 \\
\lambda_4 &= 10^{-8} \cdot \text{atan}(10^6 \cdot (x_4 - x_4^*)) \\
\lambda_5 &= 10^{-2} \\
\lambda_6 &= 1.5 \cdot 10^{-4} \cdot \frac{\frac{\partial V}{\partial x} H}{10^{-9} + \left| \frac{\partial V}{\partial x} H \right|}.
\end{aligned}$$

Notice that λ_2, λ_4 and λ_6 are tuned as saturation functions, in order to limit the control effort, without increasing too much the settling time.

The proposed solution is compared to a traditional control law based on feedback linearization (see, e.g., [29]). In this approach, the nominal error dynamics are obtained from (40) with $d = d^r = 0$, as follows

$$\ddot{y} = \ddot{r} - \ddot{r}^r = -\frac{\mu}{\|r\|^3} r + \frac{\mu}{\|r^r\|^3} r^r + u_I. \tag{41}$$

The control input vector is chosen as

$$u_I = \left(\frac{\mu}{\|r\|^3} r - \frac{\mu}{\|r^r\|^3} r^r \right) - K_p\, y - K_v\, \dot{y}, \tag{42}$$

where $K_p > 0$ and $K_v > 0$ are diagonal gain matrices. By using (42) into (41), it can be verified that this control law linearizes the nominal closed-loop system and makes the equilibrium point $y = 0$ asymptotically stable. The control gains of the three decoupled second order systems (41)-(42) have been tuned so as to reduce as much as possible the magnitude of the control input (42), while guaranteeing a settling time close to that of the proposed controller. This results in $K_p = 10^{-6} \cdot I$ and $K_v = 2 \cdot 10^{-5} \cdot I$. The selected value of K_p is such that the natural frequency of system (41)-(42) is $2\pi/T$, with T given by (11).

Table I. Initial orbital elements of the chaser and the target

Orbital element	Chaser	Target
True longitude	$L(0) = 0.0175$ rad	$L^r(0) = 0$
Semi-parameter	$p(0) = 7158$ km	$p^r(0) = 7178$ km
Eccentricity vector	$e_X(0) = 1.1 \cdot 10^{-3}$	$e_X^r(0) = 10^{-3}$
	$e_Y(0) = 0$	$e_Y^r(0) = 0$
Inclination vector	$h_X(0) = 0.313$	$h_X^r(0) = 0.315$
	$h_Y(0) = 0$	$h_Y^r(0) = 0$

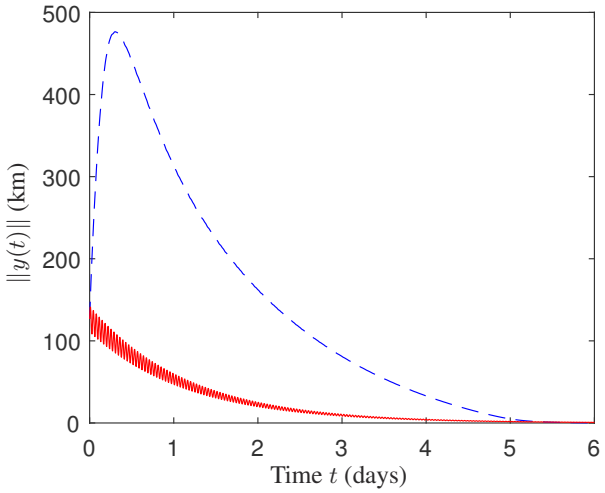

Figure 3. Relative position error magnitude obtained with the control schemes (36)-(38) (blue, dashed) and (42) (red, solid).

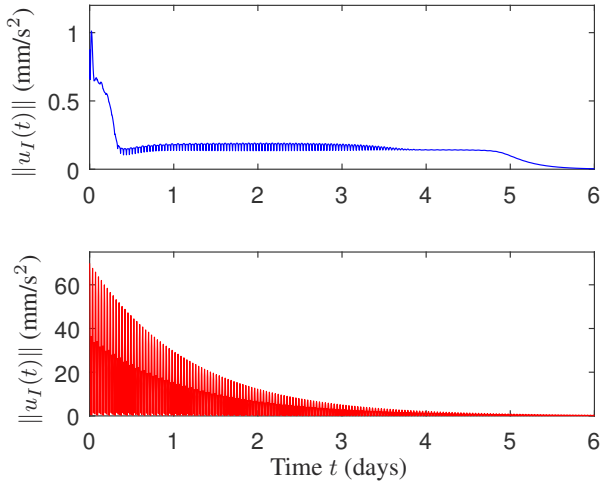

Figure 4. Magnitude of the control inputs $u_I(t)$ provided by (36)-(38) (top) and (42) (bottom).

System (40) has been numerically simulated with $d = d^r = 0$ for a time interval of approximately 6 days (corresponding to 86 orbital revolutions), using the control schemes (36)-(38) and (42). The magnitude $\|y(t)\|$ of the relative position error, resulting from the simulation, is reported in Fig. 3. Both controllers are able to keep the inter-satellite distance below 1 km, for all $t > \bar{t}$, with $\bar{t} = 5.5$ days. In Fig. 4, it can be seen that the maximum magnitude of the control input (42) is about 70 times higher than that of the input u_I corresponding to (36)-(38), which explains the two different transient behaviours in Fig. 3. Notice that, due to the nonlinear contribution between brackets in (42), it has not been possible to scale the amplitude of the control signal down to the desired level (1 mm/s^2), despite our best effort to tune the control gains K_p and K_v. In this respect, the proposed design procedure is clearly more flexible, as expected.

The true longitude tracking error $\tilde{\psi}_1(t)$ obtained with the control scheme (36)-(38) is depicted in Fig. 5. Such angle turns out to be very small even for large initial spacecraft separations. The three-dimensional profile of the trajectory of the chaser relative to the target is shown in Fig. 6 for the two controllers (note the different axis scale).

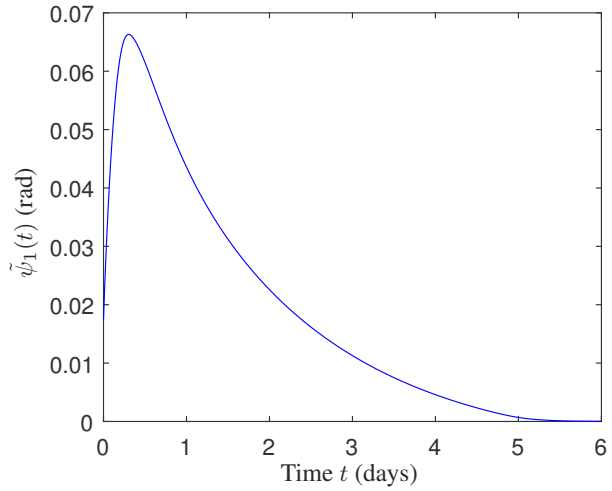

Figure 5. True longitude tracking error $\tilde{\psi}_1$, obtained with the control scheme (36)-(38).

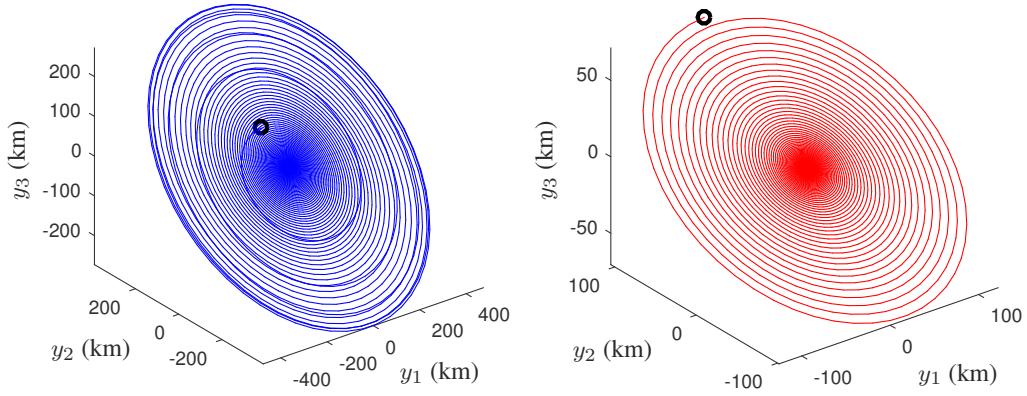

Figure 6. Relative trajectory $y(t)$ provided by the control laws (36)-(38) (left) and (42) (right), with the initial condition $y(0)$ (circled).

A qualitative assessment of the robustness of the control law (36)-(38) with respect to exogenous disturbances and parametric uncertainties has been also carried out. To this aim, the disturbance terms d and d^r in (40) have been specified so as to model the effect of the J2-harmonic of the Earth's gravity field, which is the dominant environmental disturbance in the considered scenario. Moreover, actuator scale factor and alignment errors have been included in the simulation model, by replacing the control command u (see Fig. 2) with a corrupted input $\bar{u}$ of the form

$$\bar{u}(t) = \alpha \begin{bmatrix} R(\epsilon) & 0_{2\times 1} \\ 0_{1\times 2} & 1 \end{bmatrix} u(t), \tag{43}$$

where α and ϵ denote the scale factor and alignment errors, respectively. Figure 7 depicts the closed-loop system response obtained for different values of $\alpha \in [0.9, 1.1]$ and $\epsilon \in [-0.1, 0.1]$ rad (the considered parametric intervals are in line with the typical uncertainties affecting the spacecraft actuation mechanism). It can be observed that the tracking error asymptotically converges to zero, for all parameter values in the specified range. This suggests an appreciable robustness of the design with respect to both disturbances and parametric uncertainties.

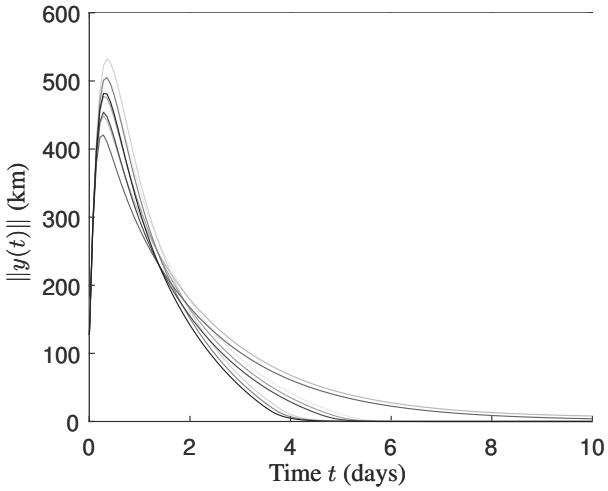

Figure 7. Relative position error magnitude obtained with the input $\bar{u}$ in (43), with $\alpha \in [0.9, 1.1]$ and $\epsilon \in [-0.1, 0.1]$.

5. CONCLUSIONS

This paper has studied the rendezvous control problem for a formation of two spacecraft orbiting about a central body. The problem is cast as that of tracking the modified equinoctial elements of a target spacecraft moving along an unperturbed closed orbit. A class of globally asymptotically stabilizing feedback control laws has been derived for this problem. They enable an actively controlled chaser spacecraft to approach and eventually dock the target. The results of a numerical case study demonstrate that the control system performance is adequate for practical implementation with low-thrust actuators. A systematic method for exploiting the proposed controller class for performance optimization is the subject of ongoing research. Robustness analysis with respect to disturbances and parametric uncertainties is another topic deserving further investigation.

References

1. D. C. Woffinden and D. K. Geller, "Navigating the road to autonomous orbital rendezvous," *Journal of Spacecraft and Rockets*, vol. 44, no. 4, pp. 898–909, 2007.
2. J. A. Starek, B. Açıkmeşe, I. A. Nesnas, and M. Pavone, "Spacecraft autonomy challenges for next-generation space missions," in *Advances in Control System Technology for Aerospace Applications*. Springer, 2016, pp. 1–48.
3. J. S. Llorente, A. Agenjo, C. Carrascosa, C. De Negueruela, A. Mestreau-Garreau, A. Cropp, and A. Santovincenzo, "PROBA-3: Precise formation flying demonstration mission," *Acta Astronautica*, vol. 82, no. 1, pp. 38–46, 2013.
4. A. A. Gonzales, C. R. Stoker, L. G. Lemke, J. V. Bowles, L. C. Huynh, N. T. Faber, and M. S. Race, "Mars Sample Return using commercial capabilities: Mission architecture overview," in *Proceedings of the IEEE Aerospace Conference*, Yellowstone, United States, 2014, pp. 1–15.
5. D. D. Mazanek, R. G. Merrill, J. R. Brophy, and R. P. Mueller, "Asteroid Redirect Mission concept: a bold approach for utilizing space resources," *Acta Astronautica*, vol. 117, pp. 163–171, 2015.
6. C. R. Hargraves and S. W. Paris, "Direct trajectory optimization using nonlinear programming and collocation," *Journal of Guidance, Control, and Dynamics*, vol. 10, no. 4, pp. 338–342, 1987.
7. F. Fahroo and I. M. Ross, "Direct trajectory optimization by a Chebyshev pseudospectral method," *Journal of Guidance, Control, and Dynamics*, vol. 25, no. 1, pp. 160–166, 2002.
8. C. Park, V. Guibout, and D. J. Scheeres, "Solving optimal continuous thrust rendezvous problems with generating functions," *Journal of Guidance, Control, and Dynamics*, vol. 29, no. 2, pp. 321–331, 2006.
9. Y. Ulybyshev, "Long-term formation keeping of satellite constellation using linear-quadratic controller," *Journal of Guidance, Control, and Dynamics*, vol. 21, no. 1, pp. 109–115, 1998.
10. M. Shibata and A. Ichikawa, "Orbital rendezvous and flyaround based on null controllability with vanishing energy," *Journal of Guidance, Control, and Dynamics*, vol. 30, no. 4, pp. 934–945, 2007.
11. G. Lantoine and R. Epenoy, "Quadratically constrained linear-quadratic regulator approach for finite-thrust orbital rendezvous," *Journal of Guidance, Control, and Dynamics*, vol. 35, no. 6, pp. 1787–1797, 2012.
12. H. Gao, X. Yang, and P. Shi, "Multi-objective robust control of spacecraft rendezvous," *IEEE Transactions on Control Systems Technology*, vol. 17, no. 4, pp. 794–802, 2009.

13. X. Gao, K. L. Teo, and G.-R. Duan, "Robust H_∞ control of spacecraft rendezvous on elliptical orbit," *Journal of the Franklin Institute*, vol. 349, no. 8, pp. 2515–2529, 2012.
14. A. Richards and J. P. How, "Robust variable horizon model predictive control for vehicle maneuvering," *International Journal of Robust and Nonlinear Control*, vol. 16, no. 7, pp. 333–351, 2006.
15. E. N. Hartley, P. A. Trodden, A. G. Richards, and J. M. Maciejowski, "Model predictive control system design and implementation for spacecraft rendezvous," *Control Engineering Practice*, vol. 20, no. 7, pp. 695–713, 2012.
16. S. Di Cairano, H. Park, and I. Kolmanovsky, "Model predictive control approach for guidance of spacecraft rendezvous and proximity maneuvering," *International Journal of Robust and Nonlinear Control*, vol. 22, no. 12, pp. 1398–1427, 2012.
17. M. Leomanni, E. Rogers, and S. B. Gabriel, "Explicit model predictive control approach for low-thrust spacecraft proximity operations," *Journal of Guidance, Control, and Dynamics*, vol. 37, no. 6, pp. 1780–1790, 2014.
18. H. Peng, J. Zhao, Z. Wu, and W. Zhong, "Optimal periodic controller for formation flying on libration point orbits," *Acta Astronautica*, vol. 69, no. 7, pp. 537–550, 2011.
19. B. Zhou, Z. Lin, and G.-R. Duan, "Lyapunov differential equation approach to elliptical orbital rendezvous with constrained controls," *Journal of Guidance, Control, and Dynamics*, vol. 34, no. 2, pp. 345–358, 2011.
20. C. A. Kluever, "Feedback control for spacecraft rendezvous and docking," *Journal of Guidance, Control, and Dynamics*, vol. 22, no. 4, pp. 609–611, 1999.
21. S. S. Vaddi and S. R. Vadali, "Linear and nonlinear control laws for formation flying," *Advances in the Astronautical Sciences*, vol. 114, pp. 171–187, 2003.
22. H. Wong, V. Kapila, and A. G. Sparks, "Adaptive output feedback tracking control of spacecraft formation," *International Journal of Robust and Nonlinear Control*, vol. 12, no. 2-3, pp. 117–139, 2002.
23. R. Pongvthithum, S. M. Veres, S. B. Gabriel, and E. Rogers, "Universal adaptive control of satellite formation flying," *International Journal of Control*, vol. 78, no. 1, pp. 45–52, 2005.
24. P. Singla, K. Subbarao, and J. L. Junkins, "Adaptive output feedback control for spacecraft rendezvous and docking under measurement uncertainty," *Journal of Guidance, Control, and Dynamics*, vol. 29, no. 4, pp. 892–902, 2006.
25. L. Sun and W. Huo, "Robust adaptive control of spacecraft proximity maneuvers under dynamic coupling and uncertainty," *Advances in Space Research*, vol. 56, no. 10, pp. 2206–2217, 2015.
26. C. Park and D. J. Scheeres, "Determination of optimal feedback terminal controllers for general boundary conditions using generating functions," *Automatica*, vol. 42, no. 5, pp. 869–875, 2006.
27. H. Peng, X. Jiang, and B. Chen, "Optimal nonlinear feedback control of spacecraft rendezvous with finite low thrust between libration orbits," *Nonlinear Dynamics*, vol. 76, no. 2, pp. 1611–1632, 2014.
28. J. A. Starek and I. V. Kolmanovsky, "Nonlinear model predictive control strategy for low thrust spacecraft missions," *Optimal Control applications and methods*, vol. 35, no. 1, pp. 1–20, 2014.
29. H. Schaub, S. R. Vadali, J. L. Junkins, and K. T. Alfriend, "Spacecraft formation flying control using mean orbit elements," *Journal of the Astronautical Sciences*, vol. 48, no. 1, pp. 69–87, 2000.
30. C. M. Kellett and L. Praly, "Nonlinear control tools for low thrust orbital transfer," in *Proceedings of the 6th IFAC Symposium on Nonlinear Control Systems*, Stuttgart, Germany, 2004.
31. M. R. Ilgen, "Low thrust OTV guidance using Lyapunov optimal feedback control techniques," *Advances in the Astronautical Sciences*, vol. 85 Part 2, pp. 1527–1545, 1993.
32. D. E. Chang, D. F. Chichka, and J. E. Marsden, "Lyapunov-based transfer between elliptic Keplerian orbits," *Discrete and Continuous Dynamical Systems Series B*, vol. 2, no. 1, pp. 57–68, 2002.
33. P. Gurfil, "Nonlinear feedback control of low-thrust orbital transfer in a central gravitational field," *Acta Astronautica*, vol. 60, no. 8, pp. 631–648, 2007.
34. T. Fossen, A. Loría, and A. Teel, "A theorem for UGAS and ULES of (passive) nonautonomous systems: Robust control of mechanical systems and ships," *International Journal of Robust and Nonlinear Control*, vol. 11, no. 2, pp. 95–108, 2001.
35. A. S. Shiriaev and A. L. Fradkov, "Stabilization of invariant sets for nonlinear systems with applications to control of oscillations," *International Journal of Robust and Nonlinear Control*, vol. 11, no. 3, pp. 215–240, 2001.
36. I. Karafyllis and J. Tsinias, "Global stabilization and asymptotic tracking for a class of nonlinear systems by means of time-varying feedback," *International Journal of Robust and Nonlinear Control*, vol. 13, no. 6, pp. 559–588, 2003.
37. M. Leomanni, G. Bianchini, A. Garulli, and A. Giannitrapani, "Nonlinear orbit control with longitude tracking," in *Proceedings of the 55th IEEE Conference on Decision and Control*, Las Vegas, United States, 2016, pp. 1316–1321.
38. M. J. H. Walker, B. Ireland, and J. Owens, "A set of modified equinoctial orbit elements," *Celestial mechanics*, vol. 36, no. 4, pp. 409–419, 1985.
39. R. H. Battin, *An introduction to the mathematics and methods of astrodynamics*. AIAA, 1999.
40. J. R. Wertz and R. Bell, "Autonomous rendezvous and docking technologies: Status and prospects," in *Proceedings of the SPIE AeroSense Symposium*, Orlando, United States, 2003, pp. 20–30.
41. R. Sepulchre, M. Jankovic, and P. V. Kokotovic, *Constructive nonlinear control*. Springer Science & Business Media, 2012.
42. S. S. Sastry, *Nonlinear systems: analysis, stability, and control*. Springer Science & Business Media, 2013.
43. S. P. Bhat and D. S. Bernstein, "A topological obstruction to continuous global stabilization of rotational motion and the unwinding phenomenon," *Systems & Control Letters*, vol. 39, no. 1, pp. 63–70, 2000.
44. M. Martinez-Sanchez and J. E. Pollard, "Spacecraft electric propulsion-an overview," *Journal of Propulsion and Power*, vol. 14, no. 5, pp. 688–699, 1998.
45. M. Leomanni, A. Garulli, A. Giannitrapani, and F. Scortecci, "Propulsion options for very low Earth orbit microsatellites," *Acta Astronautica*, 2016, doi:10.1016/j.actaastro.2016.11.001.